Journal of the Korean Vacuum Society
Vol. 4, No. 2, June 1995, pp. 124~134

〈 연구논문 〉

Development of S-band Waveguide Valve for PLS 2-GeV Linac

J. S. Bak and W. Namkung

Linac Division, Pohang Accelerator Laboratory, POSTECH, Pohang 790-784, Korea
(Received May 15, 1995)

PLS 2-GeV 선형가속기를 위한 S-band용 도파관 밸브의 개발

박주식 · 남궁원

포항가속기연구소 선형가속기부
(1995년 5월 15일 접수)

Abstract— Development of 80 MW S-band waveguide valve is now under way at Pohang Accelerator Laboratory (PAL). It is intended to have easy replacement and quick maintenance for the PLS 2-GeV linac klystrons. We adopt a new design concept which removes a limitation on power transmission. This design is completely different from the traditional one. The new S-band waveguide valve consists of the U-shaped waveguide section with a pushrod assembly, a vacuum chamber with two H-corner sections and a sealing plate with two Viton O-rings. We have achieved a high power transmission of more than 65 MW at a pulse width of 3.5 μsec and a pulse repetition frequency of 30 Hz. It also shows an excellent reliability of the vacuum seal. We report here on the design considerations, the mechanical features, and the fabrication of our first waveguide valve, the results of our experiments so far, and some of our plans for the near future.

요 약— 포항가속기연구소에서는 PLS 2-GeV 선형가속기 클라이스트론의 교체 및 보수시에 사용하기 위하여, 80 MW급 S-band의 도파관 밸브를 개발중에 있다. PLS형 도파관 밸브는 결합수단 없이 대전력을 전송할 수 있는 구조로 설계되어, 전력전송에 대한 제한을 받지 않는 특징을 갖는다. 본 도파관 밸브의 주요 구성부는 밀착구동체를 갖는 U자형 도파관부, 두개의 H-코너가 부착된 진공함, 그리고 두개의 Viton O-링이 장착된 진공기밀판으로 이루어져 있다. 시제품용 도파관 밸브의 특성조사 결과, 펄스폭 3.5 μsec, 반복율 30 Hz에서 65 MW의 전력전송을 얻을 수 있었다. 본 논문에서는 PLS 도파관 밸브의 설계 개념, 기계적 특성 및 가공의 순으로 자세히 논할 것이며, 또한 현재까지의 실험결과 및 앞으로의 계획에 대하여 보고하기도 한다.

1. Introduction

The Pohang Accelerator Laboratory (PAL) is the Korea-first comprehensive research center for accelerator technology. The facility holds the third generation synchrotron light source (Pohang Light Source, PLS) consisting of a 2-GeV electron linac and a 2-GeV electron storage ring. The outline of the PLS 2-GeV linac and its status as of 1994 are described in the previous reports [1, 2]. Since 1994 we have projected short and middle-term programs to further upgrade the PLS 2-GeV linac; extensive improvements are currently under way for the high power microwave systems such as klystron, modulator, pulse compressor, resonant ring and waveguide valve, and future facilities to promote availability of the PLS 2-GeV linac.

The PLS 2-Gev linac is a full energy injector to the storage ring which will serve as a low-em-

ittance light source for various research; basic and applied science, and industrial applications. There are 11 klystrons and modulators, and 10 SLAC-type pulse compressors in the linac gallery. In the accelerator tunnel, which is 6 m below the gallery floor, there are 42 accelerating columns, 3 beam analyzing stations, and various components to form the 150 m long linac. Installation work started on July 1, 1992 has been completed by December 10, 1993. The commissioning started on January 7, 1994. During the commissioning period of six months, we operated the machine in two stages; first without pulse compressors to obtain 1.5-GeV and then with pulse compressors for 2.0-GeV. We are now operating the machine routinely with beams of more than 2.0-GeV and 400 mA.

This study on high power waveguide valve is motivated by the requirement for more efficient maintenance and operation of the PLS 2-GeV linac. The deficiency of the waveguide valve in the waveguide network would require venting each module, each time a klystron should be replaced, and cause long interrupt of normal operation. There are two means in protecting the evacuated waveguide network from exposure to air during the replacement of high power klystron tube. Those are to use a waveguide valve or a high power rf window. At present, SLAC and IHEP adopt the waveguide valve scheme. The rf window scheme is used for the 30 MW klystron operation in KEK. Recently, JLC group in KEK developed an S-band alumina rf window for a high power transmission which exceeds 100 MW [3]. They are continuing to study about the optimization of alumina disk fabrications and long-term performance tests of a large number of windows. We expect that it is feasible for the PLS 2-GeV linac to adopt the window scheme few years later. As matters now stand, we decide to select the waveguide vacuum valve scheme based on the more conservative idea. The preliminary mechanical design for the PLS waveguide valve was completed by May 1993 under the international collaboration with Institute of High Energy Physics (IHEP), Beijing. Through the fabrication process of prototype waveguide valve, subsequent design changes were done. The basic valve configuration was the same as originally conceived, however, there were some major changes in contacting mechanism of the U-shaped waveguide and moving mechanism of the sealing plate. The shape of vacuum chamber was also modified. The fabrication of the final prototype waveguide valve was completed on November 30, 1994. The high power test started on February 20, 1995. On March 21, 1995, we attained the 65 MW power transmission with 0.12 dB insertion loss at 3.5 μsec pulse width and 30 Hz PRF. Now, we are carrying out the design change to upgrade the vacuum characteristics.

2. Design Considerations

Waveguide vacuum valves have been in use extensively and reliably at SLAC since 1968. The original SLAC type valves employed an indium vacuum sealing with knife-edge contact and a resonant iris coupling in the broad walls of the two adjacent waveguide [4]. The tightening force was provided by a lead screw actuator which is connected directly to the plunger assembly. These valves worked adequately below peak power levels of about 30 MW. However, these valves had heavily indented indium seal after many closures, then, required periodically remelting the indium to form the indium filled groove. Fig. 1 shows an assembly structure of the IHEP indium seal waveguide vacuum valve. The BEPC (Beijing Electron Positron Collider) injector linac is using the modified SLAC type waveguide valve with a deeper indium seal groove and a hemispherical sealing surface instead of a knife-edge seal. Some of these valves used in SLAC two mile linac and in BEPC injector were failed in vacuum sealing after only 3~5 times of closures due to adhesion of indium to the contact edge and heavy tear of indium seal. Moreover, the

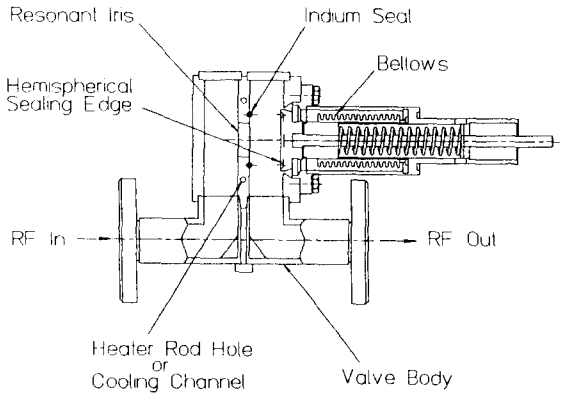

Fig. 1. IHEP indium seal waveguide valve.

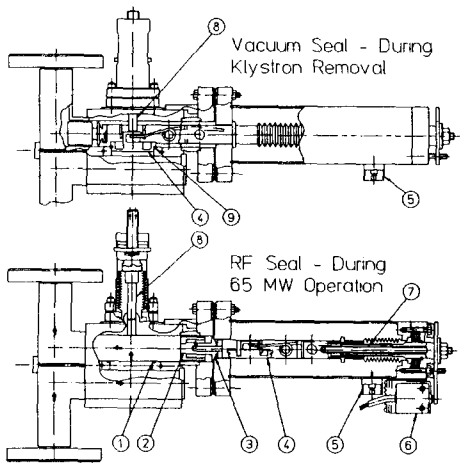

1. Resonant Iris
2. Chock Short
3. Metal-to-Metal Seal
4. O-ring Piston
5. RF Pick-up Probe
6. Microswitch
7. Drive Mechanism
8. Push Rod
9. Viton O-ring

Fig. 2. SLAC linear collider waveguide valve.

sharp jagged points come from indium adhesion caused rf breakdown during high power operation.

According to the upgrading demand for the SLAC Linear Collider (SLC), a modified waveguide valve was developed. In the new SLC design, the knife-edge indium seal was completely eliminated. The core of SLC waveguide valve design was that the indium knife-edge seal has been replaced by an O-ring seal mechanism, which was transported to a rf-free environment during high power operation. The continuity of wall currents on the contact surface was achieved through a shorted choke joint followed by a metal-to-metal rf seal. Considerable attention was given to the rf leakage into the O-ring chamber. The isolation between the high power rf region and the O-ring chamber exceeded 70 dB. The SLC type waveguide valve shown in Fig. 2 has been used for SLAC 5045 klystron with a peak rf power handling capability of 65 MW and a reliable operation of more than 200 closure cycles. Its excellent characteristics has been evidenced from the SLC operation [5].

For the PLS 2-GeV linac, we use the Toshiba E-3712 klystron with 80 MW output power at 4.4 μsec pulse width [6]. Therefore, a waveguide valve working at a peak rf power of above 80 MW is required. There are two options in establishing the principle for the PLS waveguide valve development. One is to adopt the well-proven SLC type design. Another option is to develope a completely new structural valve free from power restriction. The original SLAC and SLC type waveguide valve were designed on a basic idea using the same circular hole for rf contact and vacuum seal. However, we introduced an innovated design concept, and embodied it in a completely different structure with two WR284 rectangular contact gaskets. Fig. 3 shows a conceptual diagram of the PLS waveguide valve. Main design specifications of the waveguide valves currently in use or under development are listed in Table 1. As described in Table 1, the PLS type waveguide valve has to prepare for a highest peak power handling capability, a lowest rf leakage and a most reliable vacuum sealing. Essential design points of the PLS waveguide valve are; (1) to implement the U-shaped waveguide section for a power transmission of more than 80 MW, (2) to implement a Viton seal driving module for a reliable vacuum tight, (3) to make a good rf contact for no rf leakage, (4) to supply a clean vacuum environment for a stable operation, and (5) to adopt a robust mechanical structure for a reliable operation.

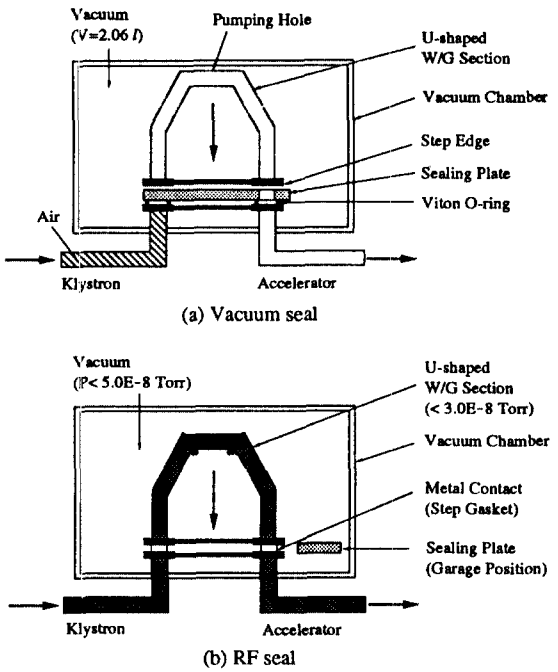

Fig. 3. Schematic diagram of the PLS waveguide valve.

3. Mechanical Features and Fabrication

Four basic factors were considered in the mechanical design. In approximate order of importance, these are; (1) precision of placement of the U-shaped waveguide section, (2) contacting property of the waveguide gaskets, (3) vacuum property of the sealing plate, and (4) reliability of the driving mechanisms.

The detailed structure of the PLS waveguide valve is shown in Fig. 4. All part drawings are found in elsewhere [7]. Materials used in the fabrication of the valve assembly are nonmagnetic. The microwave strurcture for the PLS waveguide valve is composed of an U-shaped waveguide section with two rectangular step gaskets, two H-corner sections brazed with a main vacuum chamber, and a plunger assembly for compressing two copper gaskets. It is necessary to position the U-shaped waveguide section very accurately, especially in regard to rectangular cross section of two H-corners. The motion of the U-shaped waveguide section is driven with pushrod that translates by means of 16 mm diameter screw threads. The maximum moving distance is 20 mm. In order to keep a stable horizontal motion, four grooves on inner surface of the main vacuum chamber and four spring spindles are installed. The position of the U-shaped waveguide section is adjusted and guided with connection plate and two tapered guiding pins. The gap distance between the guiding pins and holes is maintained within 10 μm. The force necessary to maintain the good rf contact and the torque on moving mechanism are 150 N/linear-cm and 15 kN-mm, respectively. In order to enhance the pushing force for the U-shaped waveguide, the driving mechanism uses the roller type bearing with tapered profile. The allowable loading force of the roller bearing is 46.5 kN. In case of excessive pressing load, the plate spring absorbs the over-pressure adequately. At a loading of 19.3 N/mm^2, the squeezed deformation of the step gasket was about 10 μm. The step gasket for rf contact is made of an annealed OFHC copper. Its thickness and Vickers hardness are 1.6 mm and 67, respectively. The protection grooves for the two

Table 1. Main specifications of waveguide valves

Type / Description	IHEP	SLAC-SLC	PLS
Peak power (MW)	30	70	80
Pulse width (μsec)	3.2	3.5	4.0
Max. repetition freq. (Hz)	50	180	60
Average power (kW)	4.8	44.2	19.2
VSWR	1.05	1.02	1.05
Insertion loss (dB)	0.08	0.1	<0.1
Max. rf leakage (W)	<2.0	<2.0	<1.0
Coupling	Resonant iris	Resonant iris	None
Open-close cycle	30	200	250
Leak rate (Torr·*l*/sec)	1.0E-8	1.0E-8	1.0E-8
RF contact seal	Indium(C)*	OFHC(C)*	OFHC(R)*
Vacuum seal	Indium	Viton	Viton

*R : Rectangular, C : Circular.

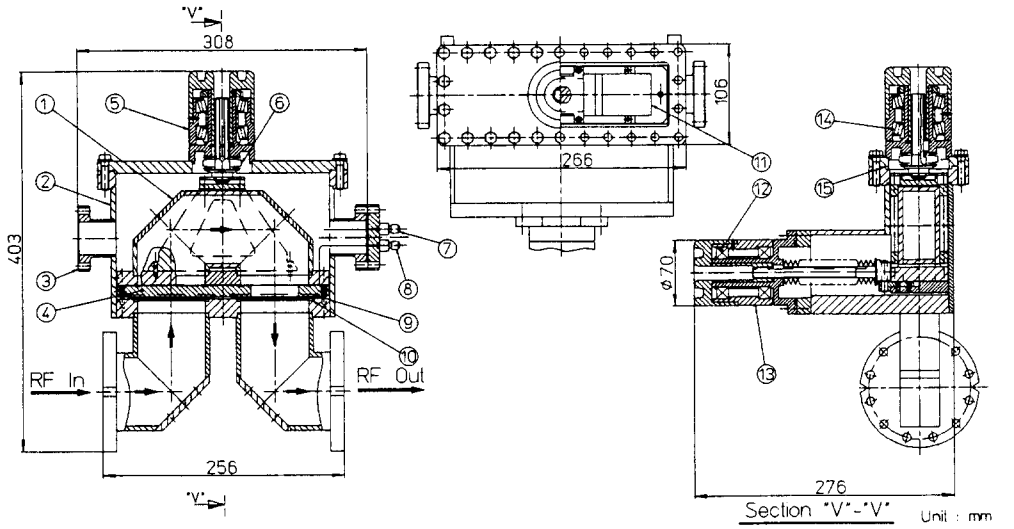

1. U-shaped W/G
2. Valve Chamber
3. Vacuum Gauge Port
4. Sealing Plate
5. Pushrod Mechanism
6. Welded Bellows
7. RF Pick-up Probe
8. Strain Gauge
9. Viton O-ring
10. Cu-Gasket
11. Rectangular Contact
12. Deep Grooved Bearing
13. Sealing Plate Driver
14. Tapered Roller Bearing
15. Silver Wire

Fig. 4. PLS 2-GeV linac waveguide valve.

rectangular step edges are carved at the top side of the sealing plate. The rectangular contacting surface of the U-shaped waveguide is made of stainless steel to provide the necessary hardness, and then is brazed onto the U-shaped copper waveguide. After brazing, the contacting surface is polished with the roughness less than 0.5 μm. The total length of the waveguide in valves is 3.3 times the guide wave length, $\lambda g = 15.3$ cm.

As with other waveguide components, waveguide vacuum valve has to meet certain vacuum-specific requirements. The requirements for vacuum valve are; (1) low outgassing rate of all parts of the valve, (2) low leak rate of the valve operating mechanism, and (3) low gas transfer leakage.

The vacuum structure for the PLS waveguide valve consists of an L-shaped vacuum chamber containing an U-shaped waveguide section, a plunger assembly and a driving module for a vacuum sealing plate. A Viton is selected as a polymer seal material considering chemical and mechanical properties, outgassing, and radiation damage. The vacuum seal between the sealing plate and bottom plate is achieved by means of two Viton O-rings and press of the U-shaped waveguide section. During the first stage, the sealing plate is brought into position and then, in the second stage, pressed against the abutment. An opening aperture of sealing plate is placed at the upstream side to prevent the valve chamber from being exposed to air during replacement of the klystron tube. Its size is set at 50×15 mm. The maximum differential pressure at opening is specified to 5.0×10^{-7} Torr. Two Viton O-rings are installed at the bottom side of sealing plate. The closed trapezium groove is used to have a very good retention of the Viton O-ring. The force pressurized on the O-ring seal is 25 N/linear-cm. The torque on the driver mechanism for vacuum sealing is 2.14 kN-mm. The O-ring compression against the rectangular seat portion should be more than 15% of the O-ring diameter. The vacuum seal for pushrod is achieved by welded bellows of 29 mm outer diameter. When the operation mode is converted from vacuum seal to rf

seal, the spring sprindles inserted in sealing plate supply the floating force to the contact surface. We have never experienced any jamming faults in moving the sealing plate. The two ports prepared at the side wall of the main vacuum chamber are used for a vacuum measuring gauge and a rf pick-up probe. The vacuum between the rectangular flange assembled with the U-shape waveguide and the vacuum chamber is sealed by silver wire with 1.5 mm diameter. After tightening bolts, this silver wire squeezes down to 0.8 mm. In order that a klystron is in operation within an allowed position of pushing rod screw, a microswitch provides a protection interlock to modulator is installed at the actuation assembly. This interlock is also linked in series to the switching terminal of vacuum gauge controller. The klystron operation is interrupted at dynamic pressure of above 2.0×10^{-8} Torr near the klystron window. The leak rate for the vacuum structure is tightly controlled to be less than 1.5×10^{-10} Torr·*l*/sec. At a power transmission mode, the evacuating volumes of the microwave pathway and the vacuum chamber garaging the sealing plate are 1.25 *l* and 2.06 *l*, respectively.

At the initial design stage, the waveguide made of stainless steel have been considered to eliminate the copper-to-stainless steel brazing process. We have calculated first theoretically the attenuation values of copper and stainless steel waveguide. Those values were 0.023 dB/m and 0.042 dB/m, respectively. Then, we have had a high power test for the sample stainless steel waveguide with a length of 587 mm. From the test results, it was found that the insertion loss of the stainless steel waveguide was more than 5 times higher than that of copper waveguide. At a peak power of 45 MW, the suface temperature on the stainless steel waveguide was increased to above 100℃ without cooling. This temperature rise can cause the damage of the O-ring seal in waveguide valve, and at the higher power level, the more power loss can be brought about. Finally, it has been concluded that the waveguide material should be OFHC copper and the copper-to-stainless steel brazing process should be overcome for the waveguide valve development.

During the early fabrication stage, we went through many difficulties for high temperature brazing. So, we describe some experiences for brazing process briefly. Our specifications required that the brazing operation takes place in an atmosphere and cleans the assembly so that no flux is required. The hydrogen atmosphere also requires that all copper in the assembly be oxygen free. Copper containing oxygen is embrittled when it comes in contact with hydrogen. In the whole brazing process, we had three independent brazing operation cycles due to different joint conditions. The B-Ag60CuIn-720, B-Ag72Cu-780 and B-Ag68CuPd-810 silver-based alloys were used as filler metals, because of their high strength, excellent corrosion and oxidation resistance, and good vacuum characteristics. The flow points were 720, 780 and 810℃. Approximately 50 grams of alloy were used. To improve the surface flow characteristics, the stainless steel joint surfaces were nickel-plated to 15 μm thickness. We used the electroless plating method to get the better uniformity of plating thickness. Placement of the alloys was found to be quite important. In most cases where tolerances would permit, the alloys were placed between parts to be joined. The shape and size of the filler metal groove were made up to contain sufficient material to fill the capillary gap at the brazing temperature. A shortfall in filler metal quantity produced gross porosity in the brazed joint and lack of bonding. The groove size was 1.5 times the maximum volume of the capillary joint by a rule of thumb. The brazing cycles were decided from the results of several trial-errors. It appeared that the brazing cycle with proper melting and cooling time had a best effect on the braze quality. Also, the furnace heating capacity was important. The copper-to-copper and copper-to-stainless steel assembly were separately run through the specified brazing cycles. Temperature

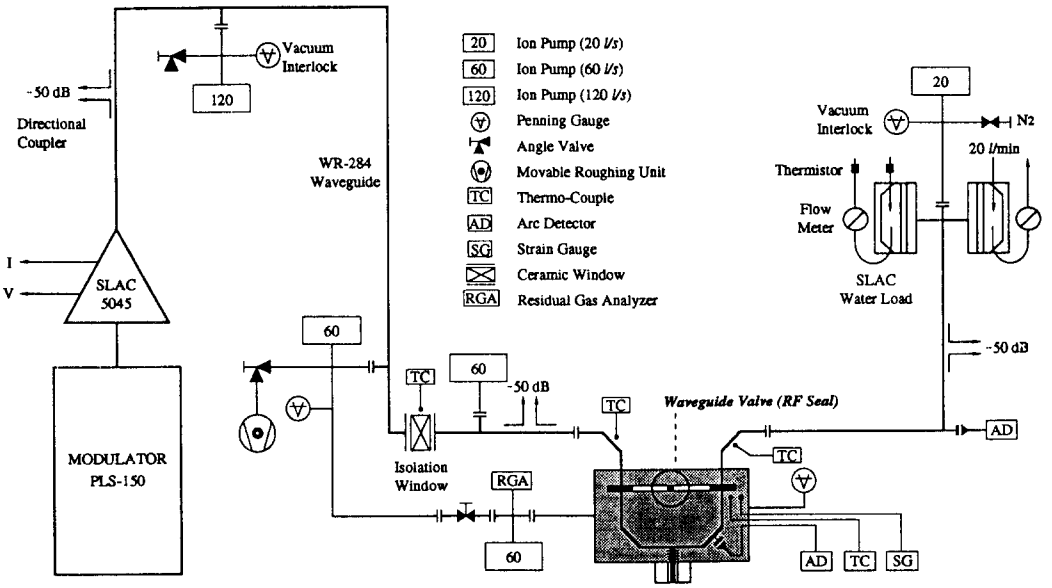

Fig. 5. Diagram of the high power test stand for the PLS waveguide valve.

was monitored by the thermocouples placed at strategic points on the assembly, and regulated by programmable controller automatically. Most of the specified requirements were met, and the braze quality was quite good. No significant changes were noted in dimensions.

4. Performance Tests

There are some possibilities for interference between the sealing plate and the U-shaped waveguide section, but no difficulty was experienced at assembly. After chemical cleaning, the prototype waveguide valve was rf cold-tested. The VSWR and insertion loss at 2856 MHz was less than 1.04 and 0.08 dB, respectively. Therefore, we didn't have any tuning operation. Then, this waveguide valve was assembled on the high power test stand. In order to shorten the rf processing time, the waveguide valve was baked *in situ* to 120℃ for 18 hr. A schematic diagram of the high power test stand is shown in Fig. 5. The 150 MW PLS prototype modulator was used for this experiment. Therefore, a pulse width was limited to 3.5 μsec. The rf output from the SLAC 5045 klystron was fed to waveguide valve, then terminated by the SLAC rf water load. The rf pulse repetition frequency was variable from 10 Hz to 30 Hz.

The evacuation system of the high power test stand with about 40 *l* in volume consisted of five sputter ion pumps with a total pumping speed of 320 *l*/sec. These pumps provided a pressure of 3.2×10^{-8} Torr in the U-shaped section and a pressure of 1.2×10^{-7} Torr in the valve chamber after initial 20 hr pumping. The vacuum pressures were monitored with cold cathode gauges and ion pump currents. The cold cathode gauges were used for vacuum interlocks. In order to protect the klystron window from a catastrophic breakdown due to bulky outgassing at the waveguide valve, a cylindrical rf window described as isolation window in Fig. 5, was inserted between the klystron window and the waveguide valve. The forward and reflected rf power in the waveguide were monitored by dual Bethe-hole couplers with a coupling ratio of −50 dB. On the outer walls of the isolation window and valve

chamber, thermocouple sensors were installed to monitor the temperature change. During the test, the vacuum pressure and the reflected power at the waveguide valve were continuously monitored, and their signals were used for interlock of klystron drive power to prevent a catastophic breakdown.

In the early stage of rf processing, at the power level less than 5 MW, the gas desorptions due to the periodic small breakdowns and occasional big breakdowns in the waveguide were inevitable. Once this stage was past, only a intermittent rise in the base vacuum pressure was observed. Based on the changes of the local pressure distribution, it was also confirmed that the frequent breakdown at low power occurred on the both side of the isolation window. From this breakdown pattern, we can estimate that the multipactor takes place severely near the isolation window. At the short pulse test of 1 μsec, the power transmission was achieved to 65 MW at 10 Hz after 196 hr of the first rf processing. The first 144 hr was spent to pass through the multipactoring region. During this first-step rf processing, the total evolved gases were about 700 μl, where the predominant gases were H_2, H_2O, CO and CO_2. In the second-step, the test began first with 25 MW power of 1.3 μsec then the pulse width and pulse repetition frequency were gradually increased to 3.5 μsec and 30 Hz, respectively. After running with 62 MW at 20 Hz, the repetition frequency was raised to 30 Hz. At 30 Hz, when the power reached 45 MW, the isolation window manufactured by IHEP was cracked and destoryed. The crack had tree-like branches with the origin at the surface. Some pitting traces on the disk surface and some arcing spots nearby copper walls were found. The center of the cracking occurred around location of the maximum E-field. From these observations, it is assumed that the crack is generated initially on the surface as a pinhole by localized thermal heating and then grows through the bulk with branching. To investigate the fundamental process of

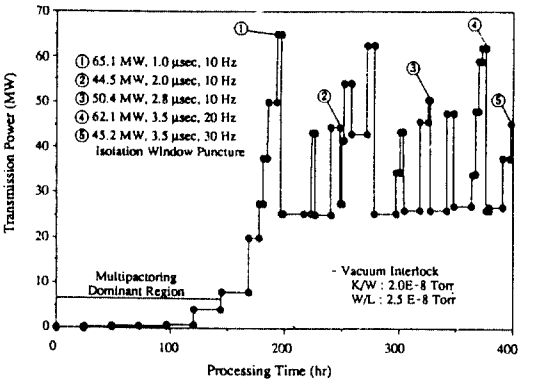

Fig. 6. First rf conditioning curve for the prototype valve.

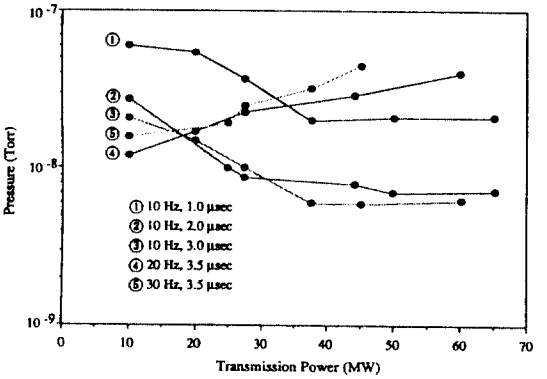

Fig. 7. Base pressure behavior at the waveguide valve.

crack generation, the spectral analysis system using an image intensifier and a monochromater is required. In this power run, the temperature rise on the isolation window frame was not higher than 13.5℃. The window frame was cooled by a forced convection air. This temperature rise was low enough to assure a reliability of the isolation window. Fig. 6 shows the first rf conditioning processed until the isolation window failure occurred. It took 380 hr to reach the power transmission of 62 MW at 3.5 μsec pulse width and 20 Hz PRF. Besides, we found a singular vacuum phenomenon in the first rf processing. Fig. 7 shows the base pressure as a function of peak power. At the pulse repetition frequency of more than 20 Hz, the base pressure slowly rises with increase of peak power. But, at 10 Hz operation,

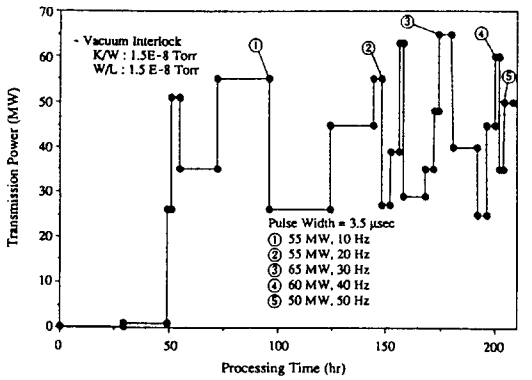

Fig. 8. Second rf conditioning curve for the prototype valve.

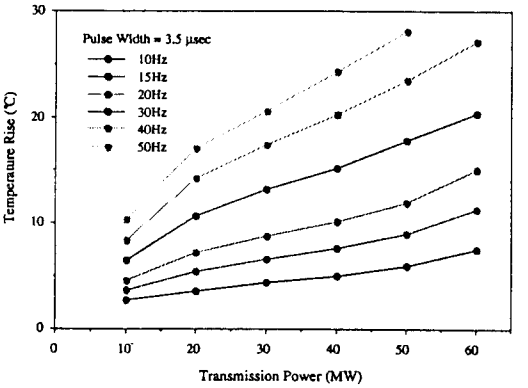

Fig. 9. Temperature rise at the U-shaped waveguide.

the base pressure has an opposite tendency against the increasing peak power. It is conjectured that this phenomenon is related to average cw power, geometrical structure and inner surface conditions of the waveguide valve, and vacuum pumping capacity, etc.

Due to the removal of the cracked isolation window, the test stand was exposed in atmosphere for 6 hr. Then it was evacuated again and started the second rf processing without isolation window. This rf conditioning was progressed very smoothly because the whole test stand was already conditioned with the high rf power. Fig. 8 is a record of the second rf processing. The pulse width was set to 3.5 μsec and pulse repetition frequency was increased from 10 Hz to 50 Hz. The vacuum interlock level was more tightly controlled to be less than 1.5×10^{-8} Torr. It took only 174 hr to obtain a transmission power 65 MW at 3.5 μsec pulse width and 30 Hz PRF. The total propagation energy required to accomplish this was more than 2 GJ. The test was continued up to 60 MW at 40 Hz, then up to 50 MW at 50 Hz.

The test was terminated at that moment. Besides, the temperature rise ΔT at the U-shaped waveguide surface was measured as a function of the transmission power. Six examples are shown in Fig. 9, which indicates that the power loss rate maintains a same level at different average cw power conditions.

In the macroscopic test, we could not find any traces of melting, micro-protrusions, crater edges, or cracks. If we adopt a more effective cleaning method, the total rf processing time for an infant waveguide valve will be within 100 hr. After the second rf processing, the base pressure in the U-shaped waveguide and the working pressure under the highest power loading were 4.6×10^{-9} Torr and 9.6×10^{-9} Torr, respectively. In addition, the average outgassing rate at the U-shaped waveguide measured by the rate-of-rise method was 8.5×10^{-12} Torr·l/s·cm^2. The continuous processing makes it possible to reduce down to about 2.0×10^{-12} Torr·l/s·cm^2. Fig. 10 shows various oscilloscope traces for the high power test. The profiles are almost flat and have no arcing traces. The transmitting power pulse was very stable under any different operation conditions. No evidence of instabilities could be observed throughout the experiment. From the power measurements by calibrated crystal detectors, when 65 MW power was transmitted to waveguide valve, the reflected power was about 1.8 MW. Thus, the mismatch loss was measured to be 0.12 dB. This power loss is about two times higher than that of the straight waveguide with equivalent length.

During the high power test, it became apparent that the vacuum improvement of the valve chamb-

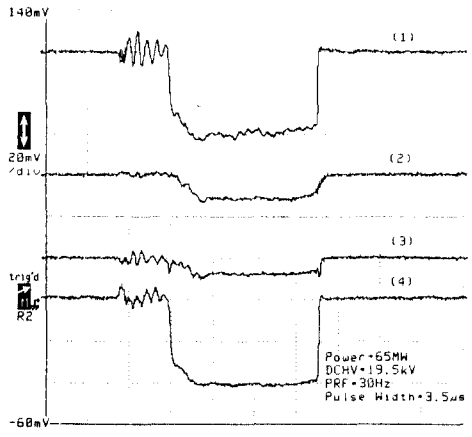

1. Waveguide Valve Forward 3. Klystron Window Reflected
2. Waveguide Valve Reflected 4. Water Load Forward

Fig. 10. Waveforms of the forward and reflected power.

er would be necessary for a reliable operation at a rf transmission mode. The holes for vacuum pumping will be implanted on both sides of the H-plane of the U-shaped waveguide to build the common pumping structure. After this modification, the separate pumping system for the waveguide valve itself will not be required, and the modified valve can serve as the vacuum pumping port on the waveguide network. In addition, as shown in Fig. 4, a rf pick-up probe to enable the monitoring of any rf leakage into the vacuum chamber and a strain gauge to check the loading force will be implemented in the valve chamber. From the proper pushing load, the maximum tolerable rf leakage into the valve chamber will be limited to 1 W peak power to avoid the Viton O-ring damage.

5. Future Works

We fabricate all components of the prototype waveguide valve in our own machining factory. According to our experience, the fabrication process can be further simplified and optimized if the available machining facilities are well equipped. We will contiune to carry out the studies on the high temperature brazing joints between different metals and the effective cleaning method for heavily oxidized Cu surfaces.

Up to now, we have the transmission test of 65 MW peak power. In order to determine the durability, higher peak power examination of the prototype valve is required. For the higher power test, we will use the 300 MW resonant ring with the power multiplication factor of 13.7 [8]. We expect that more detailed information concerning the dimension of vacuum pumping hole can be obtained from this experiment.

As stated in the previous section, we will also upgrade the vacuum characteristics of waveguide valve. To eliminate the possibility of vacuum leak and to reduce the outgassing rate significantly, the L-shaped vacuum chamber will be changed from stainless steel welding type to aluminum single body type. In addition, we will investigate concerning the reliability of closure cycles.

From the second half of this year, the revised waveguide valves will be produced and tested. The 11 valves will be installed on the PLS 2-GeV electron linac for the preventive maintenance period of next year.

6. Conclusion

A new waveguide valve has been developed for the PLS 2-GeV electron linac of the Pohang Light Soure. The power transmission of 65 MW at a pulse width of 3.5 μsec and a pulse repetition frequency of 30 Hz has been achieved by adopting the step contact structure. The present high power operation was concluded due to the modulator output power. The operating performance is very promising, no instabilies can be observed. The PLS waveguide valve is relatively simple in fabrication, stable in properties, and cheap in cost, in comparison with the existing ones. The use of the PLS waveguide valve is expected to significantly reduce the effort required to recover after klystron change and to greatly contribute in elevating the operating rate of the PLS 2-GeV linac.

Acknowledgments

The development of the PLS waveguide vacuum valve is performed as a joint project between PAL in Pohang and IHEP in Beijing. The work reported here is certainly the result of a joint effort of many people. We would like to thank Drs. Q. F. Liu and G. L. Li at IHEP for their advice and discussions concerning valve structure. We also thank Messrs. S. H. Kim, H. S. Kim and Y. J. Park for their scrupulous fabrication works and meticulous CAD drawing works. A part of the power test is carried out under a collaboration with Dr. M. H. Cho, Messrs. S. S. Park, and O. H. Hwang. Finally, the help by Mrs. S. H. Gu for chemical cleaning and Ni-plating is appreciated.

References

1. W. Namkung et al., *Commissioning of PLS 2-GeV Electron Linac*, Proc. of 1994 European Particle Accelerator Conference (London, U.K., 1994).
2. W. Namkung, *PLS 2-GeV Linac*, Proc. of the 17th Int. Linear Accelerator Conference (Tsukuba, Japan, 1994).
3. A. Miura and H. Matsumoto, *Development of an S-band RF Window for Linear Colliders*, KEK Reprint 92-215, KEK (1993).
4. A. L. Eldredge, A. J. Keicher, M. Heinz and R. J. Allyn, IEEE Trans. on Nucl. Sci. **NS-12**(3), 694 (1965).
5. N. R. Dean, W. R. Fowkes, M. W. Hoyt, H. D. Schwarz and E. F. Tillmann, IEEE Trans. on Nucl. Sci. **NS-33**, 1611 (1987).
6. M. H. Cho et al., *Performance of Pulsed High Power Klystron Tube for PLS 2-GeV Linac*, Proc. of IEEE Particle Accelerator Conference (Washington D.C., U.S.A., 1993).
7. J. S. Bak et al., *PLS 2-GeV Linac Waveguide Valve Drawing (PLW-200)*, 3rd ed. (Pohang Accelerator Laboratory, POSTECH, 1994).
8. G. N. Kim et al., *Design of High-Power Microwave Component Test Stand*, Proc. of 1994 KAPRA & KPS/DPP Joint Workshop (Daejeon, Korea, 1994).